Effect of Roller Geometry on Roller Bearing Load-Life Relation

Fred B. Oswald and Erwin V. Zaretsky
Glenn Research Center, Cleveland, Ohio

Joseph V. Poplawski
J. V. Poplawski & Associates, Bethlehem, Pennsylvania

NASA STI Program . . . in Profile

Since its founding, NASA has been dedicated to the advancement of aeronautics and space science. The NASA Scientific and Technical Information (STI) Program plays a key part in helping NASA maintain this important role.

The NASA STI Program operates under the auspices of the Agency Chief Information Officer. It collects, organizes, provides for archiving, and disseminates NASA's STI. The NASA STI Program provides access to the NASA Technical Report Server—Registered (NTRS Reg) and NASA Technical Report Server—Public (NTRS) thus providing one of the largest collections of aeronautical and space science STI in the world. Results are published in both non-NASA channels and by NASA in the NASA STI Report Series, which includes the following report types:

- TECHNICAL PUBLICATION. Reports of completed research or a major significant phase of research that present the results of NASA programs and include extensive data or theoretical analysis. Includes compilations of significant scientific and technical data and information deemed to be of continuing reference value. NASA counter-part of peer-reviewed formal professional papers, but has less stringent limitations on manuscript length and extent of graphic presentations.

- TECHNICAL MEMORANDUM. Scientific and technical findings that are preliminary or of specialized interest, e.g., "quick-release" reports, working papers, and bibliographies that contain minimal annotation. Does not contain extensive analysis.

- CONTRACTOR REPORT. Scientific and technical findings by NASA-sponsored contractors and grantees.

- CONFERENCE PUBLICATION. Collected papers from scientific and technical conferences, symposia, seminars, or other meetings sponsored or co-sponsored by NASA.

- SPECIAL PUBLICATION. Scientific, technical, or historical information from NASA programs, projects, and missions, often concerned with subjects having substantial public interest.

- TECHNICAL TRANSLATION. English-language translations of foreign scientific and technical material pertinent to NASA's mission.

For more information about the NASA STI program, see the following:

- Access the NASA STI program home page at http://www.sti.nasa.gov

- E-mail your question to help@sti.nasa.gov

- Fax your question to the NASA STI Information Desk at 757-864-6500

- Telephone the NASA STI Information Desk at 757-864-9658

- Write to:
  NASA STI Program
  Mail Stop 148
  NASA Langley Research Center
  Hampton, VA 23681-2199

NASA/TM—2015-218895

Effect of Roller Geometry on Roller Bearing Load-Life Relation

Fred B. Oswald and Erwin V. Zaretsky
Glenn Research Center, Cleveland, Ohio

Joseph V. Poplawski
J. V. Poplawski & Associates, Bethlehem, Pennsylvania

National Aeronautics and
Space Administration

Glenn Research Center
Cleveland, Ohio 44135

December 2015

Acknowledgments

Level of Review: This material has been technically reviewed by technical management.

Available from

Effect of Roller Geometry on Roller Bearing Load-Life Relation

Fred B. Oswald and Erwin V. Zaretsky[*]
National Aeronautics and Space Administration
Glenn Research Center
Cleveland, Ohio 44135

Joseph V. Poplawski
J. V. Poplawski & Associates
Bethlehem, Pennsylvania 18018

Abstract

Cylindrical roller bearings typically employ roller profile modification to equalize load distribution, minimize stress concentration at roller ends and allow for a small amount of misalignment. The 1947 Lundberg-Palmgren analysis reported an inverse fourth power relation between load and life for roller bearings with line contact. In 1952, Lundberg and Palmgren changed their load-life exponent to 10/3 for roller bearings, assuming mixed line and point contact. The effect of roller-crown profile was reanalyzed in this paper to determine the actual load-life relation for modified roller profiles. For uncrowned rollers (line contact), the load-life exponent is $p = 4$, in agreement with the 1947 Lundberg-Palmgren value but crowning reduces the value of the exponent, p. The lives of modern roller bearings made from vacuum-processed steels significantly exceed those predicted by the Lundberg-Palmgren theory. The Zaretsky rolling-element bearing life model of 1996 produces a load-life exponent of $p = 5$ for flat rollers, which is more consistent with test data. For the Zaretsky model with fully crowned rollers $p = 4.3$. For an aerospace profile and chamfered rollers, $p = 4.6$. Using the 1952 Lundberg-Palmgren value $p = 10/3$, the value incorporated in ANSI/ABMA and ISO bearing standards, can create significant life calculation errors for roller bearings.

Introduction

Classical rolling-element fatigue is the process by which repeated cycles of a concentrated compressive surface load creates surface or near-subsurface cracks that propagate into a crack network that eventually generates a spall, creating a pit in the surface of the running track. The time to failure is related to the normal load, P_n, and resultant maximum Hertz stress, S_{max}, in the contact zone and the critical shearing stresses, τ, near the surface of two bodies in contact (Ref. 1).

In 1947 Lundberg and Palmgren (Ref. 2) related rolling-element bearing life to the magnitude of the shearing stress τ, stressed volume V, depth to the critical shear stress z, and N, the number of stress cycles per inner-race revolution where for each race the life at a defined probability of survival.

$$L_{LP} \sim \left(\frac{1}{\tau}\right)^{c/m} \left(\frac{1}{V}\right)^{1/m} \frac{1}{N} (z)^{h/m} \qquad (1)$$

They chose the maximum orthogonal shear stress, τ_o as the critical shearing stress. Exponents c, m and h were chosen to fit experimental data available at that time. The rationale for the term involving z, the depth to critical shear stress, is that a significant portion of the fatigue life represents the time required for a crack to propagate to the surface and produce a fatigue spall. The life of each raceway was

---

[*]Distinguished Research Associate

$$\frac{1}{L_{10}^m} = \frac{1}{L_{10ir}^m} + \frac{1}{L_{10or}^m} \tag{2}$$

Lundberg and Palmgren (Ref. 2) related the fatigue life at a 90-percent probability of survival, L_{10}, of a radially-loaded bearing to the ratio of the load capacity of the bearing, C, and the applied load, P, to the power p. Based on test data, they established that the exponent $p = 3$ for point contact on ball bearings and $p > 3$ for line contact on roller bearings.

$$L_{10} = \left(\frac{C}{P}\right)^p \tag{3}$$

In 1952, Lundberg and Palmgren (Ref. 3) revised their load-life model for roller bearing life, based on additional experimental data. Lundberg and Palmgren stated that for line contact on both bearing races $p = 4$, while for point contact on both races $p = 3$ and they suggested that for mixed point and line contact $p = 10/3$. The ANSI/ABMA and ISO bearing life standards (Refs. 4 and 5) use the 1952 Lundberg and Palmgren relation (Ref. 3), with $p = 10/3$ for roller bearings. Bearing lives as computed according to the standards are often adjusted by means of life factors (Ref. 6) to account for longer life due to improved bearing materials, manufacturing methods and lubrication.

Zaretsky (Ref. 1) and Zaretsky et al. (Ref. 7) modified the Lundberg-Palmgren life model in Equation (1), to better fit post-1960 life data for bearings made from vacuum processed steel, which have much longer lives, particularly at light load

$$L_Z \sim \frac{1}{N}\left(\frac{1}{\tau}\right)^c \left(\frac{1}{V}\right)^{1/m} \tag{4}$$

The Zaretsky life model Equation (4), which does not include the term involving the depth to the critical shearing stress, results in a larger value of the load-life exponent p in Equation (3). Zaretsky et al. (Ref. 7) suggest that $p = 5$ is more appropriate for contemporary roller bearings with line contact where crack propagation time does not dominate bearing life. In addition, Zaretsky chose the maximum shearing stress, τ_{max} as the critical stress. This choice affects the stressed volume, since the volume is based on z_{max}, the depth to τ_{max}, which occurs at a greater depth than z_o, the depth to τ_o. A procedure for converting the life as computed from the Lundberg-Palmgren life model to the Zaretsky life model is described in Appendix B.

Either life model above can be expressed in terms of the Hertz stress, S_{max} by Equation (5), where, with line contact, exponent $n = 8$ for the Lundberg-Palmgren model of Equation (1) or $n = 10$ for the Zaretsky life model of Equation (4). Derivations for Equations (1) to (4), including an explanation of how the exponents were determined are given in Zaretsky (Ref. 1).

$$L \sim \left(\frac{1}{S_{max}}\right)^n \tag{5}$$

Although bearing researchers have long recognized that roller edge loading can significantly reduce roller bearing fatigue life, the stress concentration at the roller ends is generally not included in roller bearing life calculation. The usual procedure is to choose a roller profile that minimizes edge loading at the highest expected load and allow for a small amount of misalignment and then to ignore the effect in the life calculation, which is based on the stress at the center of the roller.

Sugiura, et al. (Ref. 8) performed rolling contact tests using fully-crowned rollers with five different values of the crown radius and four loads to find an optimal crowning that produced a stress distribution to equalize the distribution of fatigue failures between roller center and edge. They found that the effect of higher edge stresses resulted in an approximate 30 percent reduction in life when compared to the effect of the stress at the center of the contact area. This indicates that the stress at the edge of the rollers must be controlled for long bearing life.

Takata, et al. (Ref. 9) investigated both fully-crowned circular arc and optimized custom profiles on tapered roller bearings under six loading conditions, including radial and axial loads with and without misalignment to create a new design technique for optimized rollers. Fujiwara and Kawase (Ref. 10) developed an optimized logarithmic profile to exclude edge loading and maximize rolling fatigue life.

Roller crowning affects the stress distribution along the roller, increasing the maximum Hertz stress; therefore it affects the load-life and stress-life relationships. Poplawski, et al. (Refs. 11 and 12) considered the effect of crowning on roller bearing life but assumed a constant Hertz stress-life exponent in Equation (5) that did not change with different roller profiles, with $n = 8.1$ for the Lundberg-Palmgren life model and $n = 9.9$ for the Zaretsky life model.

Based on the discussion above, the objective of this work was to extend the work of Poplawski, et al. (Refs. 11 and 12) by using COBRA-AHS, a commercially-available bearing analysis code (Ref. 13) to include the effect of five roller profiles on the actual load- and stress-life relationships using both the Lundberg-Palmgren and Zaretsky bearing life models. Results are given for five different roller profiles as plots of predicted roller bearing life vs. applied radial load and vs. maximum Hertz stress. Our analysis assumes a cylindrical roller bearing with "zero" clearance in a rigid housing on a stiff shaft with no misalignment.

Nomenclature

b	semiwidth of Hertzian contact area in direction of rolling, mm (in.)
C	dynamic load capacity, N (lb)
C_i	magnitude of crown drop relief at location i, mm (in.)
C_0	roller crown drop amplitude based on a gage point along roller, mm (in.)
$C(x)$	roller crown drop at a lamina location, mm (in.)
c	stress-life exponent
d	roller diameter, mm (in.)
E	Young's modulus of elasticity, MPa (ksi)
f	ratio of ball bearing raceway groove radius to ball diameter (conformity)
h	exponent in Equation (1)
K_i	inner-race stiffness for roller lamina
k_1	constant in Equations (B1), (B2), (B3) $\text{mm}^{h/m}$ ($\text{in.}^{h/m}$)
L	life, millions of inner-race revolutions or hours
l_e	effective roller length, mm (in.)
L_B	life of bearings in gearbox, stress cycles, millions of inner race revolutions or hours
L_G	life of bearings in gearbox, stress cycles, millions of inner race revolutions or hours
L_{10}	10-percent life: life at which 90 percent of a population survives, millions of inner-race revolutions or hours
m	Weibull modulus (slope)
N	number of stress cycles per inner-race revolution
n	Hertz stress-life exponent in Equation (5) or number of lamina in Equation (13)
P, P_n	bearing, normal or roller load, N (lb)

p	load-life exponent
p_j	load acting on lamina slice i, N (lb)
R	Radius, mm (in.)
S	stress, MPa (ksi)
S_{max}	maximum Hertz stress, MPa (ksi)
V	stressed volume, mm^3 (in.^{3})
w	width of roller lamina, mm (in.)
x	dimension along roller length, mm (in.)
Y_0	roller displacement (compression) in normal direction
Z	axial location along roller
z	distance below surface to critical shear stress due to Hertzian load, mm (in.)
α	exponent
δ	deflection between axis of a finite-length cylinder and an infinite plane, mm (in.)
δ_i	deflection in roller spring element i, mm (in.)
θ	roller misalignment angle, radians
θ_a, θ_b	elastic constants for two bodies in contact
ν	Poisson's ratio
σ	stress, MPa (ksi)
τ	shear stress, MPa (psi)
τ_{max}	maximum shear stress, MPa (psi)
τ_o	maximum orthogonal shearing stress, MPa (psi)
ξ	roller lamina location, measured from roller center, mm (in.)

Subscripts:

B	bearing
G	gear
j	j_{th} lamina on roller
ir, or	inner- or outer-race of bearing
LP	refers to Lundberg-Palmgren life model, Equation (2)
max	refers to maximum Hertz stress or maximum shear stress
o	refers to maximum orthogonal shearing stress
r	residual stress
RE	rolling element set
S	shaft and inner-ring bore
s	system
x	tangential direction
Z	refers to Zaretsky life model, Equation (3)
z	normal direction

Roller Bearing Geometry

A representative cylindrical roller bearing is shown in Figure 1. The bearing comprises an inner and outer ring and plurality of rollers interspersed between the two rings and positioned by a cage or separator. The drawing shows a bearing with guiding flanges on the outer race only, which allows axial movement between the inner race and rollers.

Properties for the 210-size cylindrical roller bearings analyzed in this paper are shown in Table 1. Rollers are assumed to have a "square" cross-section, with the roller length equal to the roller diameter. Roller crowning is represented by six profiles, with profiles summarized in Table 2. The amount of crowning is expressed in terms of the maximum profile relief or "crown drop" at a "gauge point" near the ends of the rollers. The roller profiles (roller drops) for five of the profiles are plotted in Figure 2. For clarity, the scale in the vertical (crowning) direction is exaggerated by approximately 400 times compared to the horizontal direction.

The stress (or pressure) distribution across the rollers is shown for six different profiles and at three different radial loads by 18 small "thumbnail" plots in Figure 3. These plots are provided by the analysis code (Ref. 13) to help the analyst avoid excessive edge loading. The loads shown include the "reference" load of 29,190 N (6562 lb) plus a light load of 24 percent of the reference load and a heavy load of 280 percent of the reference load.

Flat (Uncrowned) Rollers

Flat rollers have a cylindrical profile of constant diameter. Flat rollers would provide pure line contact and thus the lowest contact stress. However, as shown in the top row of plots in Figure 3, flat rollers do not compensate for edge loading, which produces significant stress concentration at the ends, particularly at high loads.

Aerospace Profile

The aerospace (partially crowned) profile modeled for this paper has a flat central portion (flat length of 8.0 mm) comprising 61.5 percent of the roller length) and circular arc relief at the roller ends with a radius of curvature (1300 mm) that is 100 times the roller diameter. The stress distribution is shown in the second row of plots in Figure 3. The modification parameters were interactively chosen to control stress concentration in the middle plot. At the light load, there is no contact at the roller ends, which increases the stress at the center. Although stress concentrations appear at the roller ends at the heavy load, this stress is reduced by about 28 percent from the flat roller case.

Chamfered Profile

The chamfered (partially crowned) profile is similar to the aerospace profile. The modeled profile has a flat central portion (8.0 mm) and linear relief at the roller ends equal to the roller diameter divided by 1500. The stress distribution along the rollers (row 3 of Fig. 3) is very similar to that of the aerospace profile.

In theory, the aerospace and chamfered profiles have discontinuities in their shape: the chamfered in the slope and the aerospace in the curvature. However, in actual manufacturing practice any such discontinuities will be blended in to the flat part of the roller.

Logarithmic Profile

The logarithmic profile has a very gentle curve at the center of the roller that gradually increases, becoming theoretically infinite (tangent) at the ends. The crown drop is defined by Equation (6), where we have chosen the gauge point as 0.999 times the distance from the center to the end of a roller, this is 0.0065 mm from the ends of a 13 mm roller.

$$C(x) = C_0 \ln \left(\frac{1}{1-(2\xi/L_t)} \right)^2 \tag{6}$$

The stress distribution for the logarithmic profile modeled for this paper is shown in row 4 of Figure 3. At both the reference load and at the light load, this profile provides a more uniform stress near the roller center than any of the other profiles considered here.

Full Crowning

Fully-crowned rollers have a constant radius of curvature across the roller length, which concentrates the load and thus the contact stress towards the roller center in order to avoid loading at the roller ends. For the reference level of loading considered in this paper of 29,190 N (6562 lb), a crown radius, R equal to 150 times the roller diameter, d avoids creating stress concentration at the roller ends without excessive stress at the center of the roller. The stress distribution for this profile is shown in row 5 of Figure 3. At the heavy load, the stress distribution is similar to the preceding three profiles.

We also included more severe crowning, with $R = 100d$ to show the increased Hertz stress at the center of the rollers, particularly at lighter loads. See row 6 of Figure 3.

Laminated Roller Model

The Laminated Roller model approach to quantify the load distribution and stress pattern developed along cylinders in misaligned contact was first introduced by Daring and Radzimovsky (Ref. 14) in 1962. The method was applied to cylindrical roller bearings having crowned rollers by A.B. Jones in his early computer software (Ref. 15). The application of the laminated roller model to roller bearings is further documented by Harris (Ref. 16) in 1969. This method has been incorporated into ISO/TS 16281 (Ref. 17). The treatment of the elastic contact between the crowned roller and raceway incorporated within the software used in this study and presented in ISO/TS 16281 are both consistent with the historical publications (Refs. 14 to 16).

Anderson (Ref. 18), based on Palmgren (Ref. 19), shows that the approach (deflection) between the axis of a finite-length cylinder and an infinite plane can be expressed as:

$$\delta = 0.39 \cdot (\theta_a + \theta_b)^{0.9} \cdot P^{0.9} / l_e^{0.8} \tag{7}$$

where P is the load, l_e is the effective cylinder (roller) length, and θ is defined in terms of the elastic constants E and v as $\theta = 4(1 - v^2)/E$. The constants need not be the same for bodies a and b.

$$(\theta_a + \theta_b) = 4 \left[\frac{(1-v_a^2)}{E_a} + \frac{(1-v_b^2)}{E_b} \right] \tag{8}$$

Solving for the force P and substituting for $(\theta_a + \theta_b)$ gives

$$P = \frac{l_e^{8/9} \cdot \delta^{10/9}}{4 \cdot (0.39)^{10/9} \left[\dfrac{1-\upsilon_a^2}{E_a} + \dfrac{1-\upsilon_b^2}{E_b} \right]} = \frac{0.7117 \cdot l_e^{8/9} \delta^{10/9}}{\left[\dfrac{1-\upsilon_a^2}{E_a} + \dfrac{1-\upsilon_b^2}{E_b} \right]} \tag{9}$$

Defining the stiffness $K = P/\delta^\alpha$ (recall that for line contact, $\alpha = 10/9 \approx 1.11$), gives

$$K = \frac{0.7117 \cdot l^{8/9}}{\left[\dfrac{1-\upsilon_a^2}{E_a} + \dfrac{1-\upsilon_b^2}{E_b} \right]} \tag{10}$$

If bodies a and b are the same material, the denominator of Equation (10) simplifies to $2(1 - v^2)/E$.

Dareing and Radzimovsky (Ref. 14) introduced a method to estimate the load distribution across a misaligned roller (cylinder). In their model, the roller was approximated as a series of n thin disks or lamina where each lamina is of width w (Fig. 4). The shear stress between adjacent lamina disks due to the variation of load along the roller was neglected. Since this method is an approximation, the laminated roller model cannot predict stress concentration such as at the edge of a roller contact.

The rolling-element bearing analysis code (Ref. 13) used for the analysis in this paper embodies both the laminated roller model (Ref. 14) and a method based on the numerical approach of Hartnett (Ref. 20) to calculate the contact stresses between a profiled roller and raceway. The more rigorous approach of Hartnett (Ref. 20) yields stress concentration estimates not available from the laminated roller approach. Experimental validation of the Hartnett methodology was presented by Hartnett and Kannel in Reference 21.

The load distribution along a loaded and misaligned roller to raceway contact can be determined by representing the lamina to raceway contact with an equivalent spring (Fig. 5). The stiffness of the i_{th} equivalent lamina spring can be determined from applying the line-contact load/deflection relationship of Equation (10), replacing the roller width, l, with the lamina width, w:

$$K = \frac{0.7117 \cdot w^{8/9}}{\left[\dfrac{1-\upsilon_a^2}{E_a} + \dfrac{1-\upsilon_b^2}{E_b} \right]} \tag{11}$$

The force p_j in a roller lamina becomes:

$$p_j = K_j w^{8/9} \delta_j^{10/9} \tag{12}$$

From Figure 5, the compression, δ_i within each of the n lamina springs can be calculated for small angles of misalignment, θ as:

$$\delta_j = Y_0 + Z\theta - 2C_j \tag{13}$$

Misalignment is not considered in this paper, therefore, $\theta = 0$ in Figure 5. The compression force in the lamina spring element, p_j is found from the displacement, δ_j using Equation (13). The total roller load P_{ir} at a particular location is found by summing the individual lamina forces, p_j as shown in Equation (14). For equilibrium, the roller loads must equal the applied loads on the bearing.

$$P = \sum_{j=1}^{n} p_j \qquad (14)$$

The equations above apply to both the inner and outer race contacts.

The fatigue life estimates presented by the authors use the classical Lundberg-Palmgren (L-P) life models since the authors do not accept the fatigue limit stress life method contained in ISO/TS 16281 (Ref. 17). Furthermore, that method has not been accepted in the United States per the American Bearing Manufacturers Association ANSI/ABMA-11:1990 (Ref. 4). Therefore, the load-life exponent using the L-P life model will not be a variable as implied by the fatigue limit stress life approach.

Finally, the software incorporates the method for calculating the life of the inner and outer raceways and combining those into a bearing life as is consistent with the original L-P approach and used within ISO/TS 16281 (Ref. 17).

Results and Discussion

Analysis

A commercial rolling-element bearing analysis code (Ref. 13) was used to calculate the fatigue lives, maximum Hertz stresses at the inner- and outer-race and the depth to the maximum shearing stress for radially-loaded cylindrical roller bearings with 50-mm bore in 1910-, 110-, 210-, and 310-size and for 30-mm bore, 1906-size and 100 mm bore, 220-size bearings. This paper shows the results for only the 210-size bearings. The calculations were performed for six loads for each of the five roller profiles. The analysis assumed a cylindrical roller bearing with "zero" clearance in a ridged housing on a stiff shaft with no misalignment.

The code can analyze the effect of typical roller profiles on bearing stress and life. Lives predicted by the code, which is based on Lundberg and Palmgren theory (Refs. 2 and 3), were adjusted for the Zaretsky (Refs. 1 and 7) life model for comparison with the Lundberg-Palmgren results. The Weibull slope for roller bearings was taken to be $m = 1.125$.

The reference roller profile for this paper has an aerospace profile with flat length (8.0 mm) comprising 61.5 percent of the roller length and with a radius of curvature (1300 mm) that is 100 times the roller diameter. These parameters were chosen interactively in the analysis software to avoid stress concentration at the ends of the rollers for the reference load of 29,190 N (6562 lb). The reference load produces an inner-ring maximum Hertz stress of 2240 MPa (325 ksi) with the aerospace profile. The computed stress distribution across the roller width at the reference load for each of the six roller profiles is shown in Figure 3.

Six load cases ranging from 6,940 to 81,994 N (1,560 to 18,443 lb) were chosen for the analysis. These loads produced inner-ring maximum Hertz stress ranging from 1200 to 3620 MPa (174 to 525 ksi) for the aerospace profile. The loads and resulting maximum Hertz stresses are given in Table 3 for each of the 36 cases analyzed.

Effect of Roller Profile

The effect of roller profile on life for the six load cases for six profiles is shown in Figure 6. For each profile, the computed life is plotted vs. the applied load to produce a load-life plot. The longest computed life at any load would be produced by flat rollers (where stress concentration at roller ends was neglected). For flat rollers, the load life exponent $p = 4$ from Equation (3), which is in agreement with the Lundberg-Palmgren life model. Crowning decreases the effective roller length and increases the maximum stress at the center of the roller, which decreases the life, particularly at light loads.

At the highest load in Figure 6, for the most severe crowning, where $R = 100d$, the life is 17 percent less than the calculated life for flat rollers. At the lightest load, the life is reduced much more, by 86 percent compared to flat rollers. The greater effect at light loads is reflected in the load-life exponent p, which is reduced from $p = 4$ for flat rollers to $p = 3.1$ with severe crowning. This case was included to show the effect of excessive crowning. For the more moderate full crown, where $R = 150d$, the load-life exponent $p = 3.2$. The analysis shows that the 1952 assumption by Lundberg and Palmgren (Ref. 3) of a load life exponent of $p = 10/3$ (or 3.33) applies only to crowned rollers.

The chamfered profile and the similar aerospace profile have a very similar stress distribution (Fig. 2) and produce almost identical load-life curves (Fig. 6). A full crown with crown radius 150 times roller diameter also avoids stress concentration at the ends but at the expense of higher stress at the roller center and thus lower life because of the greater crown drop.

The life data of Figure 6 were replotted in Figure 7 to show the relationship between maximum Hertz stress and life. For flat rollers, the load life exponent $c = 8$ in Equation (1), which agrees with the Lundberg-Palmgren life model. Because crowning increases the Hertz stress at the center of the rollers, the stress at each condition differs for the various profiles. As shown in Figure 6, increased crowning will decrease life. However, because crowning increases stress at the center of the rollers, the Hertz stress-life exponent n increases with crowning instead of decreasing. Note that the two fully crowned profiles (crown radius, $R = 150d$ and $R = 100d$) produce approximately the same value of exponent $n = 8.8$ even though these profiles have different values of the load-life exponent p (see Fig. 6).

The load-life relation for both the Lundberg-Palmgren (Refs. 2 and 3) and Zaretsky (Refs. 1 and 7) life models is compared in Figure 8 for three roller profiles. With the Zaretsky model, the load-life exponent $p = 5.0$ for a flat profile. An aerospace profile reduces the load-life exponent to $p = 4.6$. The full crown reduces the exponent further, to $p = 4.3$. With an aerospace crown, the Zaretsky model (where $p = 4.6$) yields lives ranging from 5 to 45 times the lives predicted by the Lundberg-Palmgren model (where $p = 3.5$) for the range of loads shown.

Figure 9 shows the same life data from the Zaretsky model as Figure 8 except the vertical axis shows the maximum Hertz stress, rather than the applied radial load. As in Figure 7, roller crowning increases the stress-life exponent, c, from 10.1 for flat rollers to 10.8 for fully crowned rollers according to the Zaretsky life model.

The calculated load-life exponent, p and the Hertz stress-life exponent, n for radially-loaded 210-size roller bearings are summarized in Table 4 for each of the five roller profiles analyzed in this paper. For flat rollers, $n = 8.0$ for the Lundberg-Palmgren model and $n = 10.1$ for the Zaretsky model, which nearly agree with the values 8.1 and 9.9 assumed in Poplawski, et al. (Refs. 11 and 12). However, as the crown drop increases, the exponent n becomes greater than the constant values assumed in Reference 12.

In addition to the results for 210-size bearings described herein, a similar life analysis was conducted for 50-mm bore bearings in 1910-, 110- and 310-size and for 30-mm bore, 1906-size and 100-mm bore, 220-size cylindrical roller bearings. Computed results (not shown in this paper) for the load-life exponent, p and the stress-life exponent, n were identical to results given in Table 4 for 210-size bearings.

Roller Bearing Field Data

The application of both the Lundberg-Palmgren model and the Zaretsky model to predict roller life and reliability need to be benchmarked and verified under a varied load and operating profile. The cost and time to laboratory test a statistically significant number of roller bearings of different roller geometries to determine their life and reliability is prohibitive. A practical solution to this problem is to benchmark the analysis to field data. Fortunately, these data were available for a commercial turboprop gearbox (Ref. 22).

Field data were collected for 64 new commercial turboprop gearboxes. From these field data, the resultant time to removal of each gearbox is presented in the Weibull plot of Figure 10. The failure index was 59 out of 64. That is, 59 out of the 64 gearboxes removed from service were considered failed. For these data, there was no breakdown of the cause for removal or the percent of each component that had

failed. The resultant L_{10} life from the field data was 5627 hr and the Weibull slope m was 2.189. The lowest lived components in the gearbox are the roller bearings. As a result, the Weibull slope assumed for the planetary gear spherical roller bearings is assumed to be the Weibull slope m of the entire gearbox system. Using the Lundberg-Palmgren model the predicted L_{10} life was 774 hr and the Weibull slope m was 1.125. The field data suggest that the L_{10} life of the gearbox was under predicted by a factor of 7.56 (Ref. 22).

Although errors in the assumed operating profile of the gearbox may account for the difference between actual and predicted life, it is suggested that using the Lundberg-Palmgren equations results in a life prediction that is too low for the bearings.

With reference to Equation (3), in their 1952 publication (Ref. 3), Lundberg and Palmgren proposed a load-life exponent $p = 10/3$ for roller bearings, where one raceway has point contact and the other raceway has line contact. The 10/3 load-life exponent has been incorporated in the ANSI/ABMA (Ref. 4) and ISO (Ref. 5) standards first published in 1953. Their assumption of point and line contact may have been correct for many types of roller bearings in use at that time. However, it is no longer the case for most roller bearings manufactured today, and most certainly not for cylindrical roller bearings. The analysis employed for the bearing life calculations used a value of $p = 3$ for ball bearings and $p = 4$ for roller bearings. Poplawski, Peters, and Zaretsky (Refs. 11 and 12) suggest the use of $p = 4$ for ball bearings and $p = 5$ for roller bearings (Ref. 22).

From (Ref. 22), the Weibull plot of Figure 10 showing the predicted life of the gearbox, has a Weibull slope or modulus, $m_{sys} = 1.125$. It was based on Weibull slopes for roller bearings of $m_B = 1.125$ (Lundberg and Palmgren (Ref. 3)). And, from experimental data (Ref. 23), the Weibull modulus (slope) m_G of gears equals 2.5.

The Weibull plot of the field data in Figure 10 for the lives of the turboprop gearboxes contained 59 failures out of 64 gearboxes. These failures were ~90 percent the result of planetary bearing failures, less than 2 percent from gear failures and the balance from other bearing failures (Ref. 22). The resulting Weibull slope or modulus of the gearbox failures m_s was 2.189. It is assumed that the Weibull modulus (slope) of the gearbox system is the same as that of the shortest-lived components in the system, which are the planetary bearings. Hence, the Weibull modulus (slope) of the bearings m_B was assumed also to be 2.189. From Reference 23, the Weibull slope m_G of the gears, from experimental data, was assumed to be 2.5. From Strict Series Reliability (Appendix A),

$$\frac{1}{L_{sys}^{m_s}} = \frac{1}{L_B^{m_B}} + \frac{1}{L_G^{m_G}} \tag{15a}$$

and substituting in the known values

$$\frac{1}{(5627)^{2.189}} = \frac{1}{L_B^{2.189}} + \frac{1}{(16,680)^{2.5}} \tag{15b}$$

and solving for the bearing system life, results in a value of

$$L_B = 5627 \text{ hr} \tag{15c}$$

From Lundberg-Palmgren (Ref. 2), the predicted bearing system life is

$$L_B \sim \left(\frac{C_D}{P_{eq}}\right)^4 \sim 774 \text{ hr} \tag{16a}$$

then,

$$\left(\frac{C_D}{P_{eq}}\right) \sim 5.27 \tag{16b}$$

Calculating a revised value for the load-life exponent p for the gearbox bearings based on the actual bearing system life of 5627 hr,

$$\left(\frac{C_D}{P_{eq}}\right)^p \sim (5.27)^p \sim 5627 \text{ hr} \tag{17a}$$

Solving for load-life exponent p,

$$p = 5.2 \tag{17b}$$

For line contact (roller bearing) the Hertz stress-life exponent $n = 2p$. From Equation (17b), $n = 10.4$ for line contact for the turboprop gearbox data. Referring to the Zaretsky model, Equation (4), for line contact the shear stress-life exponent is

$$c = n - \frac{1}{m} \tag{18a}$$

and where $n = 10.4$ and $m = 2.189$,

$$c = 10.4 - \frac{1}{2.189} = 9.943 \tag{18b}$$

Using the value of c from Equation (18b) to solve for the Hertz stress-life exponent n for point contact where m is assumed to equal 1.11, then

$$n = c + \frac{2}{m} = 9.943 + \frac{2}{1.11}$$
$$= 11.74 \tag{19a}$$

and for point contact,

$$p = \frac{n}{3} = \frac{11.74}{3} = 3.91 \tag{19b}$$

The apparent load-life exponent p for the roller bearings is equal to 5.2 and correlates with the Zaretsky model. Were the roller bearing lives to be recalculated using a load-life exponent $p = 5.2$, the predicted L_{10} life of the gearbox would be equal to the actual life obtained in the field, 5627 hr. It should be noted that if an exponent $p = 5$ were used; the predicted L_{10} life of the gearbox would be 4065 hr. This result suggests a strong reliance of the predicted bearing life upon the load-life exponent p and correlates with reasonable engineering certainty with the analysis of the load-life relation for the Zaretsky life model shown in Figure 8. The values of the load-life exponent p for roller bearings equal to 10/3 from the ANSI/ABMA and ISO standards (Refs. 4 and 5) and 4 from computer codes may provide predicted roller bearing lives that are too conservative for design purposes.

Summary of Results

A commercial bearing analysis code (Ref. 13) was used to calculate the fatigue lives for radially-loaded cylindrical roller bearings with five different roller profiles. Lives predicted by the code, which is based on the Lundberg-Palmgren life model (Refs. 2 and 3), were adjusted to also predict roller bearing life based on the Zaretsky (Refs. 1 and 7) life model. The following results were obtained.

1. The Zaretsky life model for rollers with an aerospace or chamfered crown predicts roller bearing life between 5 and 45 times the life predicted by the 1952 Lundberg and Palmgren model depending on load. The Zaretsky model better fits post-1960 bearing life data for vacuum processed steel bearings.

2. The Zaretsky life model produces a load-life exponent $p = 5$, for flat (uncrowned) rollers if stress concentration effects at the ends of the rollers is neglected. This compares with $p = 4$ for the Lundberg-Palmgren theory with flat rollers.

3. Using the Zaretsky life model, the load-life exponent p is reduced from 5.0 for flat rollers to 4.6 for either aerospace or chamfered rollers and to 4.3 for fully-crowned rollers.

4. The analysis shows that the 1952 assumption of Lundberg and Palmgren of a load life exponent of $p = 10/3$ applies only to crowned rollers. Using the Lundberg-Palmgren life theory, the load-life exponent is reduced from a value of 4 for flat rollers to approximately 10/3 for fully-crowned rollers.

Appendix A.—Derivation of Strict Series Reliability

As discussed and presented in Reference 11 and 23, G. Lundberg and A. Palmgren (Ref. 2) in 1947, using the two parameter Weibull equation for rolling-element bearing life analysis, first derived the relationship between individual component lives and system life. The following derivation is based on but is not identical to the Lundberg-Palmgren analysis (Ref. 1).

The two parameter Weibull equation which is a cumulative distribution function can be written as

$$\ln \ln \left[\frac{1}{S_{\text{sys}}} \right] = m \ln \left[\frac{L}{L_\beta} \right] \tag{A1}$$

where L is the number of cycles to failure, S_{sys} is the system probability of survival; m is the Weibull modulus or slope designating the type of distribution, e.g., where $m = 1$, exponential distribution, 2, Raleigh distribution, and 3.57, Gaussian or normal distribution; and L_β is the characteristic life or the life at a 63.2 percent probability of failure (Ref. 1).

Figure 11 is a sketch of multiple Weibull plots where each Weibull plot represents a cumulative distribution of each component in the system. The system Weibull plot represents the combined Weibull plots 1, 2, 3, and so forth. All plots are assumed to have the same Weibull slope m.

The slope m can be defined as follows:

$$m = \frac{\ln \ln \left[\dfrac{1}{S_{\text{sys}}} \right] - \ln \ln \left[\dfrac{1}{S_{\text{ref}}} \right]}{\ln L - \ln L_{\text{ref}}} \tag{A2a}$$

or

$$\frac{\ln \left[\dfrac{1}{S_{\text{sys}}} \right]}{\ln \left[\dfrac{1}{S_{\text{ref}}} \right]} = \left[\frac{L}{L_{\text{ref}}} \right]^m \tag{A2b}$$

From Equations (A1) and (A2b),

$$\ln \left[\frac{1}{S_{\text{sys}}} \right] = \left[\ln \frac{1}{S_{\text{ref}}} \right] \left[\frac{L}{L_{\text{ref}}} \right]^m = \left[\frac{L}{L_\beta} \right]^m \tag{A3}$$

and

$$S_{\text{sys}} = \exp - \left[\frac{L}{L_\beta} \right]^m \tag{A4}$$

where $S_{\text{sys}} = S$ in Equation (A1). For a given time or life L, each component or stressed volume in a system will have a different reliability S. For a series reliability system

$$S_{\text{sys}} = S_1 \cdot S_2 \cdot S_3 \cdot \ldots \tag{A5}$$

Combining Equations (A4) and (A5) gives

$$\exp-\left[\frac{L}{L_\beta}\right]^m = \exp-\left[\frac{L}{L_{\beta 1}}\right]^m \times \exp-\left[\frac{L}{L_{\beta 3}}\right]^m \times \ldots \tag{A6a}$$

$$\exp-\left[\frac{L}{L_\beta}\right]^m = \exp-\left\{\left[\frac{L}{L_{\beta 1}}\right]^m + \left[\frac{L}{L_{\beta 2}}\right]^m + \left[\frac{L}{L_{\beta 3}}\right]^m + \ldots\right\} \tag{A6b}$$

It is assumed that the Weibull slope m is the same for all components. From Equation (A6b)

$$-\left[\frac{L}{L_\beta}\right]^m = -\left\{\left[\frac{L}{L_{\beta 1}}\right]^m + \left[\frac{L}{L_{\beta 2}}\right]^m + \left[\frac{L}{L_{\beta 3}}\right]^m + \ldots\right\} \tag{A7a}$$

Factoring out L from Equation (B7a) gives

$$\left[\frac{1}{L_\beta}\right]^m = \left[\frac{1}{L_{\beta 1}}\right]^m + \left[\frac{1}{L_{\beta 2}}\right]^m + \left[\frac{1}{L_{\beta 3}}\right]^m + \ldots \tag{A7b}$$

From Equation (A3) the characteristic lives $L_{\beta 1}$, $L_{\beta 2}$, $L_{\beta 3}$, etc., can be replaced with the respective lives L_1, L_2, L_3, etc., at S_{ref} (or the lives of each component that have the same probability of survival S_{ref}) as follows:

$$\left[\ln\frac{1}{S_{\text{ref}}}\right]\left[\frac{1}{L_{\text{ref}}}\right]^m = \left[\ln\frac{1}{S_{\text{ref}}}\right]\left[\frac{1}{L_1}\right]^m + \left[\ln\frac{1}{S_{\text{ref}}}\right]\left[\frac{1}{L_2}\right]^m + \left[\ln\frac{1}{S_{\text{ref}}}\right]\left[\frac{1}{L_3}\right]^m + \ldots \tag{A8}$$

where, in general, from Equation (A3)

$$\left[\frac{1}{L_\beta}\right]^m = \left[\ln\frac{1}{S_{\text{ref}}}\right]\left[\frac{1}{L_{\text{ref}}}\right]^m \tag{A9a}$$

and

$$\left[\frac{1}{L_{\beta 1}}\right]^m = \left[\ln\frac{1}{S_{\text{ref}}}\right]\left[\frac{1}{L_1}\right]^m, \text{etc.} \tag{A9b}$$

Factoring out ln $(1/S_{\text{ref}})$ from Equation (A8) gives

$$\left[\frac{1}{L_{\text{ref}}}\right] = \left\{\left[\frac{1}{L_1}\right]^m + \left[\frac{1}{L_2}\right]^m + \left[\frac{1}{L_3}\right]^m + \ldots\right\}^{1/m} \qquad \text{(A10)}$$

or rewriting Equation (A10) results in

$$\left[\frac{1}{L}\right]^m = \sum_{i=1}^{n}\left[\frac{1}{L_i}\right]^m \qquad \text{(A11)}$$

Equation (A11) is identical to Equations (2) and (15a) of the text.

Appendix B.—On Converting Calculated Life From the Lundberg-Palmgren Life Model to the Zaretsky Life Model

Zaretsky et al. (Ref. 7) modified the equation for the Lundberg-Palmgren bearing life model (Refs. 2 and 3), by making three changes: (1) replacing the orthogonal shear stress with the maximum shear stress; (2) eliminating the dependence on the Weibull modulus (slope), m in the first term (which involves the shear stress, τ) and (3) removing the term involving the depth to critical shear stress.

If we solve for the life for the life L_Z from the Zaretsky model Equation (3) in terms of the Lundberg-Palmgren life, L_{LP}, Equation (2), we have:

$$L_Z = k_1 \left(L_{LP}\right) \left(\frac{\tau_o}{\tau_{max}}\right)^c \left(\frac{V_{LP}}{V_Z}\right)^{1/m} \left(\frac{1}{z_o}\right)^{h/m} \tag{B1}$$

Constant k_1 incorporates the dimension of $z^{h//m}$, where z is the depth to the critical shear stress. The value of k_1 is unknown. The value of k_1 will vary with different units of z. In this paper, we assume that k_1 is unity when z is expressed in mm. For z in inches and with line contact, where exponent $h/m = 2.071$, the value converts to $k_1 = (1 / 25.4)^{2.071} = 0.001232$. It will take a series of life tests to establish the actual value of this constant.

For roller bearings with line contact, the maximum orthogonal shear stress $\tau_o = 0.25 S_{max}$, while the maximum shear stress, $\tau_{max} = 0.300 S_{max}$ and S_{max} is the maximum Hertz stress. Therefore the ratio $\tau_o/\tau_{max} = 0.25/0.300 = 0.833$.

The Lundberg-Palmgren life model is semi-empirical. The exponents for the various terms were chosen to fit the experimental data available at the time. In their 1952 paper (Ref. 3), they show the Weibull slope for ten roller bearing tests, with thirty bearings in each test. The test bearings included tapered, cylindrical and spherical roller bearings. The exponents varied from 0.7 to 1.4. Thus, they stated "The value $e = 10/9$ can be taken as a mean value as with ball bearings."

Lundberg and Palmgren *(3)* adjusted their exponents in order to have an integer value for p, the load/life exponent, where $p = (c-h+1)/(2m)$. For roller bearings with line contact, they chose $m = 9/8$ which makes $p = 4$.

Lundberg and Palmgren (Refs. 2 and 3) chose for their exponent involving the critical shearing stress in Equation (1) $c = 10.33$ for either ball bearings or roller bearings Therefore, for roller bearings with line contact, where $L \sim 1/\tau^{c/m}$, $c/m = 10.33/1.125 = 9.182$.

When he modified the life relation, removing the dependence on the Weibull slope, Zaretsky adjusted the exponent c so that it is equal to the published values of the Lundberg-Palmgren quotient c/m. This exponent will not vary if the Weibull exponent is changed from the nominal value. Therefore, for roller bearings, the term $(\tau_o/\tau_m)^c = (0.833)^{9.182} = 0.1875$.

The stressed volume in either life model is the product of the circumference of the rolling-element running track, times the width of the contact times the depth to the critical shear stress. In changing from the orthogonal to maximum shear stress, the only parameter for the stressed volume that changes is the depth to the critical shear stress.

The maximum shear stress occurs at greater depth than the maximum orthogonal shear stress; therefore, z_m is greater than z_o. For cylindrical roller bearings, $z_o = 0.5b$, while $z_m = 0.786b$, where $b = $ the half-width of the Hertzian contact stress zone and the Weibull slope $m = 1.125$. Therefore, the term $(V_{LP}/V_Z)^{1/m} = (z_o/z_m)^{1/m} = (0.50/0.786)^{1/1.125} = 0.6689$.

To remove the dependence on the depth to the critical shear stress for the Zaretsky (Z) life model, the LP life is divided by $z_o^{h/m}$, where for line contact, the exponent $h/m = 2.33/1.125 = 2.071$. For roller bearings with line contact, Equation (B1) simplifies to Equation (B2)

$$L_Z = k_1 \left(L_{LP}\right) \left(0.1875\right) \left(0.6689\right) \left(\frac{1}{0.5b}\right)^{2.071} = k_1 \left(L_{LP}\right) \left(0.1254\right) \left(\frac{1}{0.5b}\right)^{2.071} \qquad \text{(B2)}$$

For ball bearings, with $m = 1.11$, $c/m = 10.33/1.11 = 9.306$. The term $(\tau_o/\tau_m)^c = (0.785)^{9.306} = 0.1056$. For ball bearings with typical conformity, $f = 0.52$, $z_o = 0.49b$ while $z_m = 0.767b$. Thus, $(V_{LP}/V_Z)^{1/m} = (0.49/0.767)^{1/1.11} = 0.6679$.

As above, to remove the dependence on the depth to the critical shear stress for the Zaretsky (Z) life equation, the LP life is divided by $z_o^{h/m}$, where for point contact, $h/m = 2.33/1.11 = 2.099$. Thus, for ball bearings with point contact, Equation (B1) simplifies to Equation (B3)

$$L_Z = k_1 \left(L_{LP}\right) \left(0.1056\right) \left(0.6689\right) \left(\frac{1}{0.49b}\right)^{2.0991} = k_1 \left(L_{LP}\right) \left(0.07054\right) \left(\frac{1}{0.49b}\right)^{2.0991} \qquad \text{(B3)}$$

References

1. Zaretsky, E.V. (2010), "Rolling Bearing Life Prediction, Theory, and Application," *Recent Developments in Wear Prevention, Friction and Lubrication*, 2010: ISBN: 978-81-308-0377-7, George K. Nikas, ed. Research Signpost, Kerala, India, 2010, pp. 45–136 (also NASA/TP—2013-215305).

2. Lundberg, G., and Palmgren, A., (1947), "Dynamic Capacity of Rolling Bearings," *Acta Polytechica, Mechanical Engineering Series*, 1, 3, Stockholm, Sweden.

3. Lundberg, G.; and Palmgren, A., (1952), "Dynamic Capacity of Roller Bearings," *Handlingar Proceedings,* No. 210, The Royal Swedish Academy of Engineering Sciences, Stockholm Sweden.

4. ANSI/ABMA–11:1990. R2008 (2008), *Load Ratings and Fatigue Life for Roller Bearings*, American Bearing Manufacturers Association, Washington, DC.

5. International Organization for Standardization (ISO), (2007), *Rolling Bearings—Dynamic Load Ratings and Rating Life*, ISO 281:2007, International Organization for Standardization, Geneva, Switzerland.

6. Zaretsky, E.V., ed. (1999), *STLE Life Factors for Rolling Bearings*, STLE SP-34, 2nd edition, Society of Tribologists and Lubrication Engineers, Park Ridge, IL. ISBN 9993313599, ISBN 13: 9789993313595.

7. Zaretsky, E.V., Poplawski, J.V. and Peters, S.M. (1996), "Comparison of Life Theories for Rolling-Element Bearings," *Tribology Transactions*, 39, 2, pp. 237–247.

8. Sugiura I., Ito S., Tsushima N., and Muro H., (1982), "Investigation of Optimum Crowning in a Line Contact Cylinder-to-Cylinder Rolling Contact Fatigue Test Rig," ASTM STP 771, pp. 136–149, J.J.C. Hoo, ed., American Society for Testing and Materials, Philadelphia, PA.

9. Takata, H., Suzuki, S. and Maeda, E., (1992), "Experimental Study of Fatigue Life of Profiled Roller Bearings," NSK Technical Journal, 653, pp. 1–7.

10. Fujiwara, H. and Kawase, T., (2006), "Logarithmic Profiles of Rollers in Roller Bearings and Optimization of the Profiles," NTN TECHNICAL REVIEW No. 75 (2007), reprinted from the original paper (in Japanese) *Proceedings of the Japan Society of Mechanical Engineers* Part C, 72 (2006), pp. 3022–3029.

11. Poplawski, J.V., Peters, S.M., and Zaretsky, E.V., (2001), "Effect of Roller Profile on Cylindrical Roller Bearing Life Prediction—Part I: Comparison of Bearing Life Theories, STLE Tribology Trans., 44, 3, pp. 339–350.

12. Poplawski, J.V., Peters, S.M., and Zaretsky, E.V., (2001), "Effect of Roller Profile on Cylindrical Roller Bearing Life Prediction—Part II: Comparison of Roller Profiles, 44, 3, pp. 417–427.

13. Poplawski, J.V., Rumbarger, J.H., Peters, S.M., Flower, R., and Galaitis, H. (2002) "Advanced Analysis Package for High Speed Multibearing Shaft Systems: COBRA-AHS," Final report, NASA Contract NAS3–00018.

14. Dareing, D.W. and Radzimovsky, E.I., (1962), "Influence of Misalignment on Roller Bearing Loads and Bearing Life Expectancy," Jersey Production Research Company, Tulsa, OK.

15. Jones, A.B., (1964), Personal Communication between A.B. Jones and J.V. Poplawski, Pratt & Whitney Aircraft, East Hartford, CT, November, 1964.

16. Harris, T.A., (1969) "The Effect of Misalignment on the Fatigue Life of Cylindrical Roller Bearings Having Crowned Rolling Members," *Trans. ASME*, JOLT, 91, No. 2, 1969, pp. 294–300.

17. International Organization for Standardization (ISO), (2008), ISO/TS 16281:2008, "Rolling Bearings—Methods for Calculating the Modified Reference Rating Life for Universally Loaded Bearings," International Organization for Standardization, Geneva, Switzerland.

18. Anderson, W.J. (1964), "Rolling-Element Bearings," *Advanced Bearing Technology*, E.E. Bisson and W.J. Anderson, eds., NASA SP–38, National Aeronautics and Space Administration, Washington, DC, pp. 164–168.

19. Palmgren, A. (1959), *Ball and Roller Bearing Engineering*, Third ed., SKF Industries, Philadelphia, PA.

20. Hartnett, M.J., (1979), "The Analysis of Contact Stresses in Rolling Element Bearings," *ASME Journal of Lubrication Technology*, 101, 1 Jan. 1979, pp. 105–109.

21. Hartnett, M.J. and Kannel, J.W., (1981), "Contact Stresses Between Elastic Cylinders-A Comprehensive Theoretical and Experimental Approach," *Journal of Lubrication Technology*, 103, No. 1, pp. 40–45.

22. Zaretsky, E.V., Lewicki, D.G., Savage, M., and Vlcek, B.L., (2007), "Determination of Turboprop Reduction Gearbox System Fatigue Life and Reliability," Tribology Trans., 50, 4, pp. 507–516.

23. Melis, M.E., Zaretsky, E.V., and August, R., (1999), "Probabilistic Analysis of Aircraft Gas Turbine Disk Life and Reliability," J. Propulsion and Power, Trans. AIAA, 15, pp. 658–666.

Table 1.—Bearing properties

Bearing description	Bore, mm	Outside diameter, mm	Number of elements	Roller diameter, d		Roller length	
				mm	in.	mm	in.
210-size cylindrical roller bearing	50	90	10	13	0.5118	13	0.5118

TABLE 2.—ROLLER PROFILE PARAMETERS

Profile	Flat length	Radius of curvature	Drop at gauge point, mm	Max. deflection at ref load, mm
Flat (no crown)	13 mm (100%)	n/a	n/a	0.0355
Full crown, R = 150d	0.0 (0%)	1950 mm	0.010812	0.0443
Full crown, R = 100d	0.0 (0%)	1300 mm	0.016218	0.0484
Chamfered	8.0 mm (61.5%)	n/a	0.008677	0.0395
Aerospace	8.0 mm (61.5%)	1300 mm	0.010064	0.0398
Logarithmic	0.0 (0%)	n/a	0.020000	0.0401

TABLE 3.—LOAD LEVELS AND CORRESPONDING INNER-RACE MAXIMUM HERTZ STRESS, MPa (ksi)
FOR CYLINDRICAL ROLLER BEARINGS WITH FIVE ROLLER PROFILES AT SIX LOAD LEVELS

Profile	Radial load, N (lbf)					
	6,940 (1,560)	15,980 (3,592)	20,100 (4,519)	29,190 (6,562)	58,780 (13,214)	81,994 (18,433)
Flat (no crown)	1025 (149)	1556 (226)	1745 (253)	2102 (305)	2984 (433)	3534 (513)
Full crown, R = 150d	1406 (204)	1883 (273)	2052 (298)	2376 (345)	3200 (464)	3716 (539)
Full crown, R = 100d	1507 (219)	2011 (292)	2178 (316)	2496 (362)	3300 (479)	3806 (552)
Chamfered	1200 (174)	1713 (248)	1891 (274)	2232 (324)	3086 (448)	3614 (524)
Aerospace	1200 (174)	1720 (249)	1900 (276)	2240 (325)	3092 (448)	3620 (525)
Logarithmic	1240 (180)	1730 (251)	1910 (277)	2250 (326)	3110 (451)	3620 (525)

TABLE 4.—LOAD-LIFE AND HERTZ STRESS-LIFE EXPONENTS FOR A
CYLINDRICAL ROLLER BEARING WITH RADIAL LOAD

Profile	Lundberg-Palmgren Life Model		Zaretsky Life Model	
	Load-life exp., p	Stress-life exp., n	Load-life exp., p	Stress-life exp., n
Flat (no crown)	4.0	8.0	5.0	10.1
Full crown, R = 150d	3.2	8.8	4.3	10.8
Full crown, R = 100d	3.1	8.8	4.1	10.8
Chamfered	3.5	8.2	4.6	10.3
Aerospace	3.5	8.2	4.6	10.3
Logarithmic	3.7	8.2	4.6	10.5
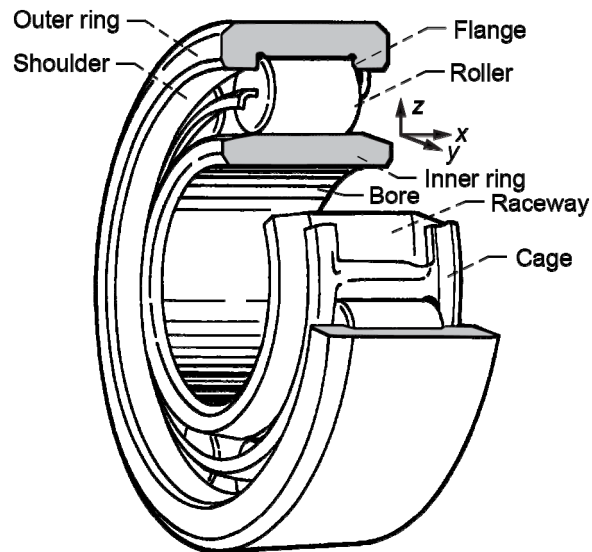
Figure 1.—Schematic of cylindrical roller bearing.

Full crown, R = 100 d
Full crown, R = 150 d
Aerospace
Chamfered
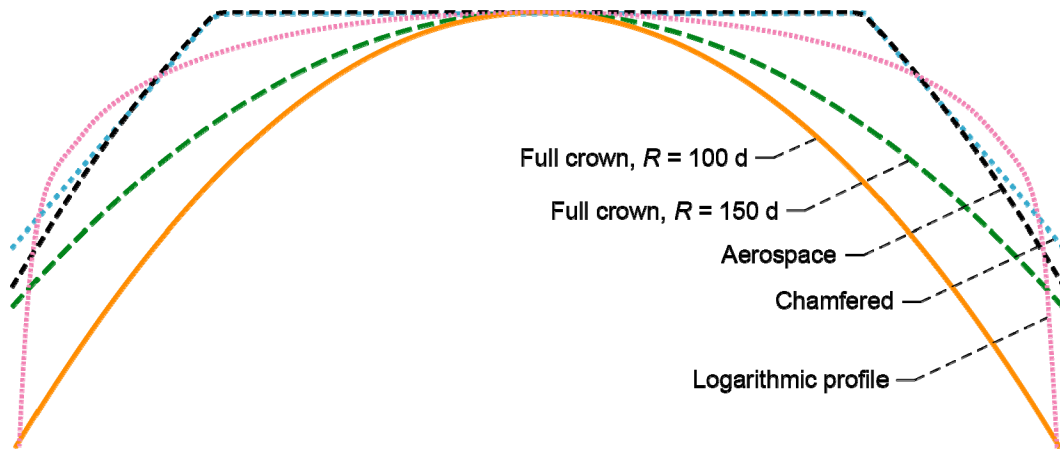Logarithmic profile

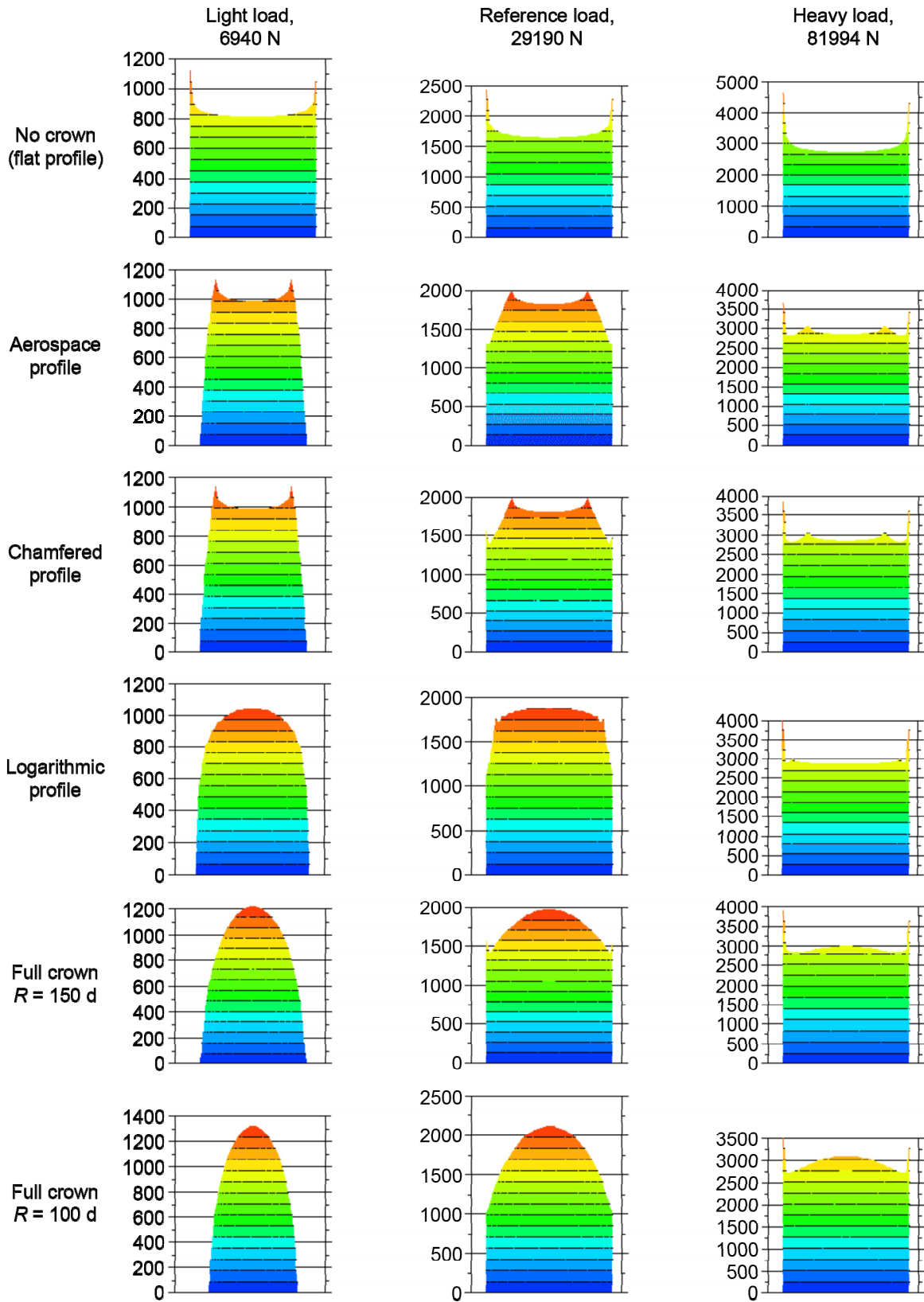Figure 2.—Crown drop (vertical dimension exaggerated) for various roller profiles.

Figure 3.—Comparison of stress distribution across rollers at three load levels for various roller profiles. (The ordinate to each figure is the contact stress in MPa across the axial length of the roller profile shown in the abscissa).
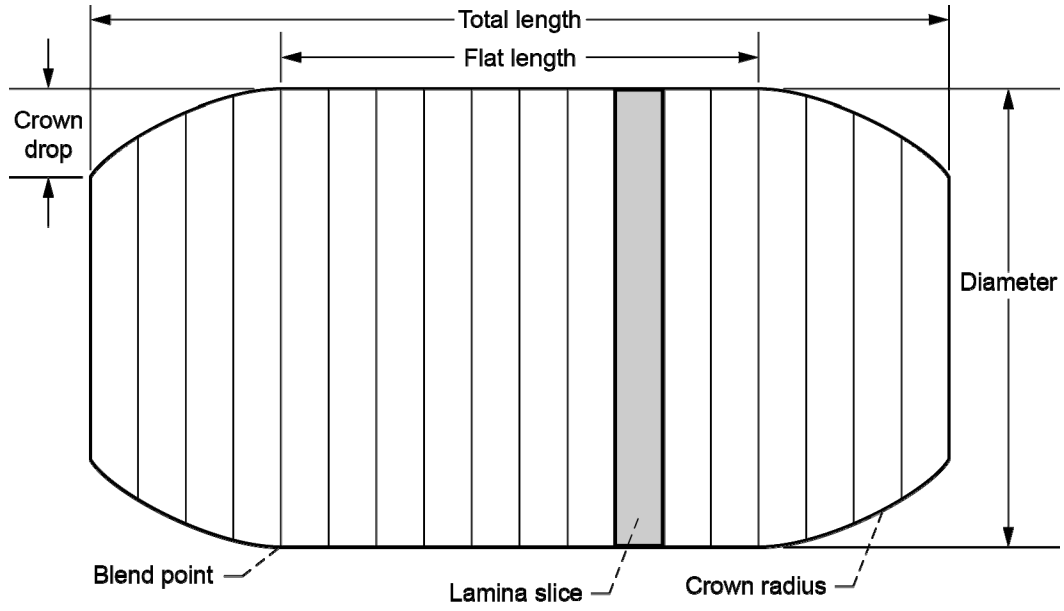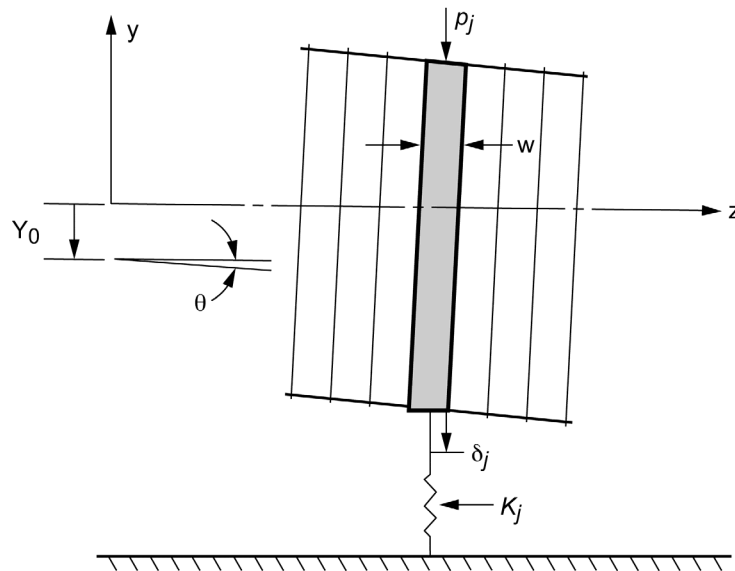
Figure 4.—Lamina representation of a roller.
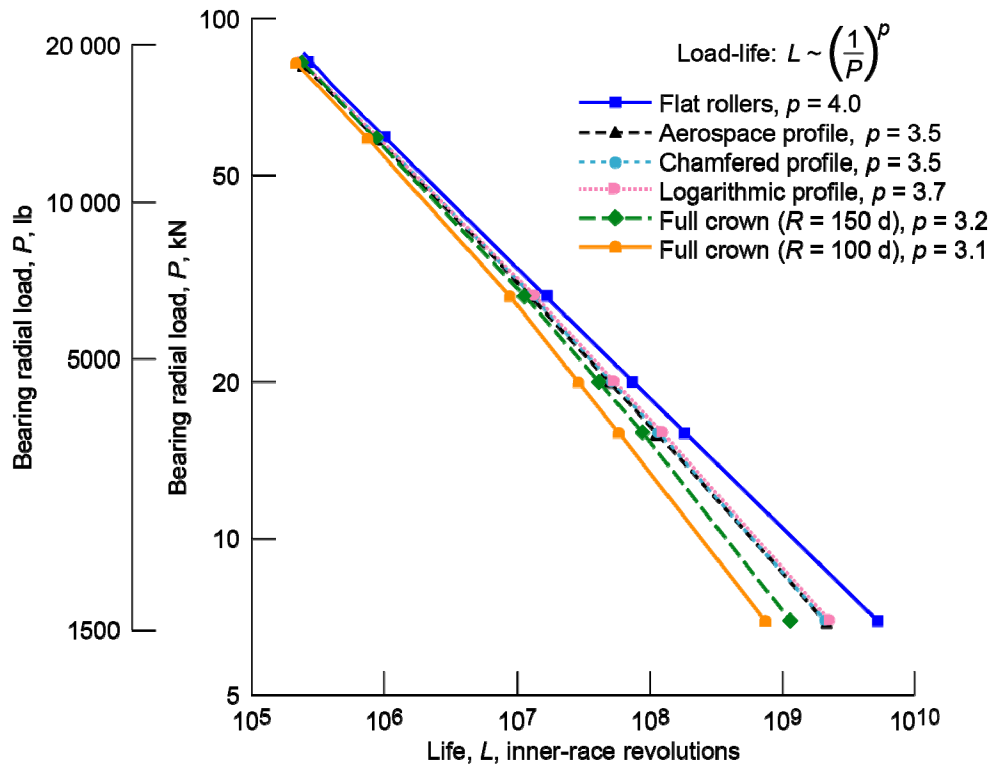

Figure 5.—Lamina to raceway equivalent spring.

Figure 6.—Effect of six roller profiles on roller bearing life and load-life relationship according to the Lundberg-Palmgren life model for a 50-mm bore, cylindrical roller bearing.
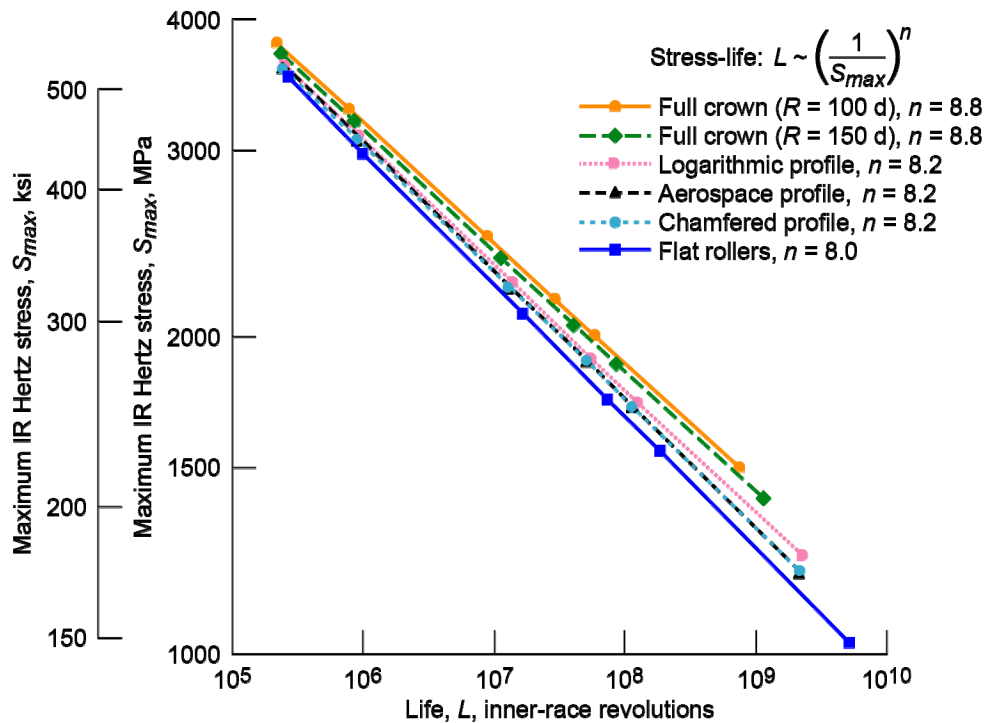
Load-life: $L \sim \left(\frac{1}{P}\right)^p$

Flat rollers, $p = 4.0$
Aerospace profile, $p = 3.5$
Chamfered profile, $p = 3.5$
Logarithmic profile, $p = 3.7$
Full crown ($R = 150$ d), $p = 3.2$
Full crown ($R = 100$ d), $p = 3.1$

Figure 7.—Effect of six roller profiles on roller bearing life and Hertz stress-life relationship according to the Lundberg-Palmgren life model for a 50-mm bore, cylindrical roller bearing.

Stress-life: $L \sim \left(\frac{1}{S_{max}}\right)^n$

Full crown ($R = 100$ d), $n = 8.8$
Full crown ($R = 150$ d), $n = 8.8$
Logarithmic profile, $n = 8.2$
Aerospace profile, $n = 8.2$
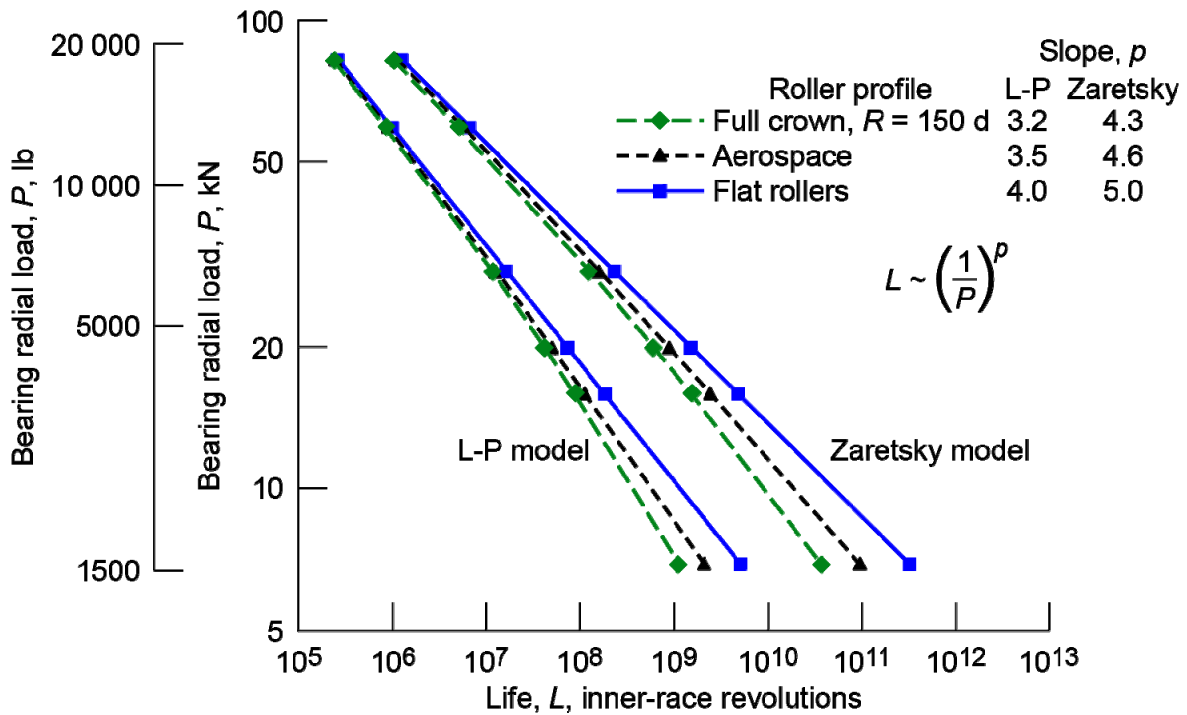Chamfered profile, $n = 8.2$
Flat rollers, $n = 8.0$

Figure 8.—Comparison of Lundberg-Palmgren and Zaretsky life models for roller bearing life and load-life relationship for a 50-mm bore, cylindrical roller bearing with three roller profiles.
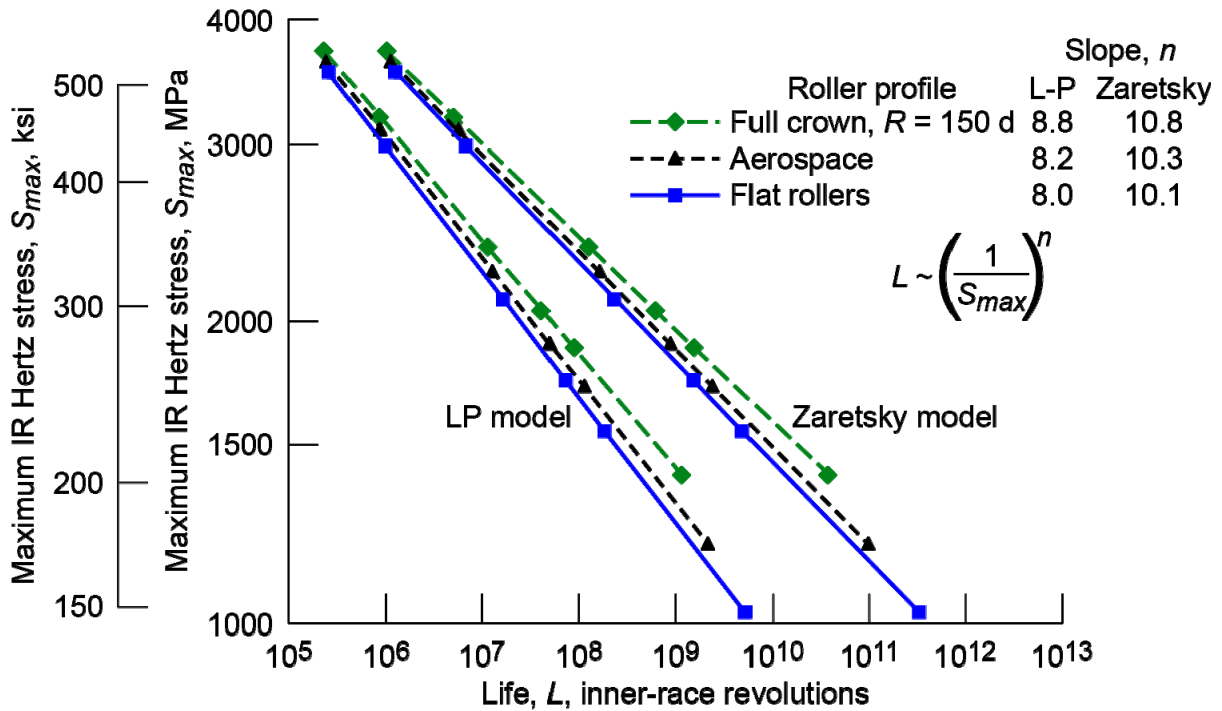

Figure 9.—Comparison of Lundberg-Palmgren and Zaretsky life models for roller bearing life and Hertz stress-life relationship for a 50-mm bore, cylindrical roller bearing with three roller profiles.
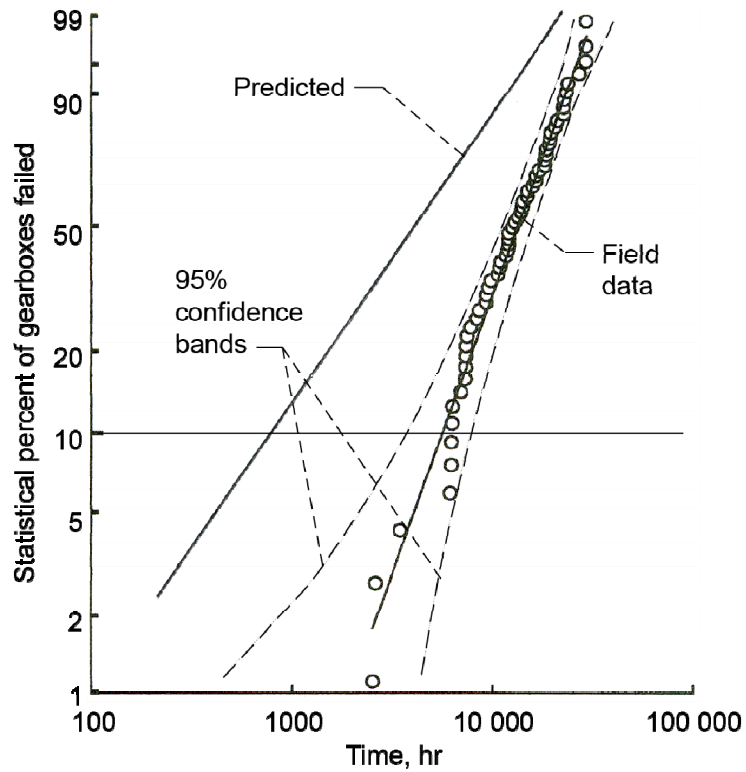
Figure 10.—Weibull plot of field data for lives of turboprop gearboxes compared with predicted lives using Lundberg-Palmgren life model. Failure index, 59 out of 64 (Ref. 22).
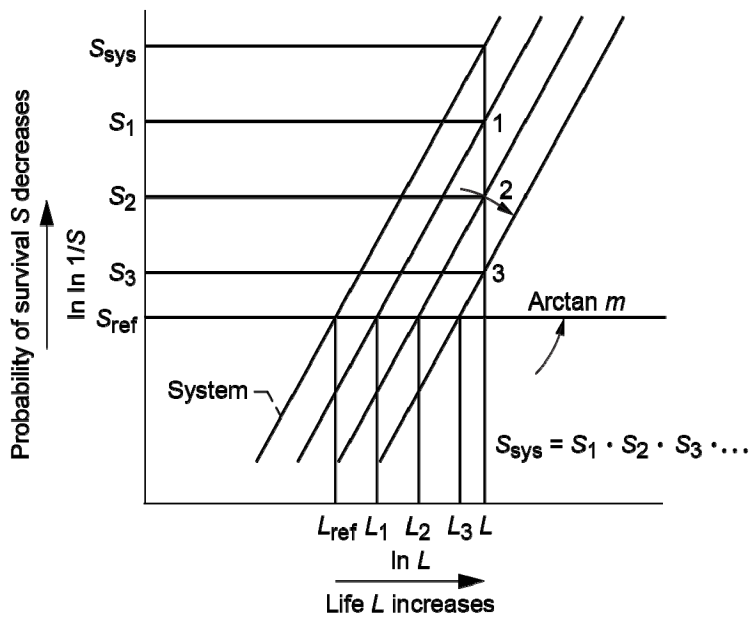

Figure 11.—Sketch of multiple Weibull plots where each numbered plot represents cumulative distribution of each component in system and system Weibull plot represents combined distribution of plots 1, 2, 3, etc. (all plots are assumed to have same Weibull slope m) (Ref. 11).